

NUMERICAL STUDY OF THE MECHANICAL BEHAVIOUR AND DAMAGE OF FGM BENT PIPES UNDER INTERNAL PRESSURE AND COMBINED BENDING MOMENT

Amin HOUARI*¹, Kouider MADANI**², Salah AMROUNE***³
 Leila ZOUAMBI**², Mohamed ELAJRAMI**²

*Faculty of Technology, Department of Mechanical Engineering, University of M'hamed Bougara, Boumerdes 35000, Algeria

**Faculty of Technology, Department of Mechanical Engineering, University of Djilali Liabes SBA, Sidi Bel Abess, 22000, Algeria

***Faculty of Technology, Department of Mechanical Engineering, University of Mohamed Boudiaf-M'Sila, M'sila, 28000, Algeria

a.houari@univ-boumerdes.dz, koumad10@yahoo.fr, salah.amroune@univ-msila.dz
zouambileila@yahoo.com, eladjrami_mohamed@yahoo.fr

received 15 February 2023, revised 25 April 2023, accepted 4 May 2023

Abstract: The main objective of this work is the numerical prediction of the mechanical behaviour up to the damage of the bends of the functionally graded material (FGM) type ceramic/metal pipes. Firstly, the effective elastoplastic proper-ties of bent FGM pipes were determined using the homogenisation law by the Mori–Tanaka models for the elastic part and TTO (Tamura-Tomota-Ozawa) for the plastic part based on a rule of mixtures per function in the form of a power law. Our work also aims at the use of a meshing method (UMM) to predict the behaviour of the FGM by finite element in the mesh of the model. The analysis was performed using the UMM technique for different loading cases and volume fraction distribution. Two stages are necessary for the analysis of the damage: the first is the model of initiation of the damage established by the criterion of maximum deformation named MAXPE and the second is criterion of the energy of the rupture according to the theory Hillerborg used to determine damage evolution. Both stages involve a 3D finite element method analysis. However, for damage, the XFEM technique was used in our UMM method to predict crack initiation and propagation in FGM pipe bends. The results of the numerical analysis concerning the mechanical behavior showed, that if the nature of the bent pipes is in FGM, a good reduction of the various stresses compared to those where the nature of the pipe is metallic material. The results were presented in the form of a force–displacement curve. The validation of the proposed numerical methodology is highlighted by comparisons of current results with results from the literature, which showed good agreement. The analysis took into account the effect of the main parameters in a bent FGM pipe under internal pressure and bending moment on the variation of the force–strain curves.

Key words: FGM, ceramic/metal, elbow pipe, internal pressure, bending moment, MMU technique

1. INTRODUCTION

Hollow cylinders and thick-walled cylindrical shells are common components used in structural applications and device systems involving aerospace structures and civil engineering structures, machinery, pipes, probes and petrochemical structures (1). These structures, mainly consisting of straight pipes and elbows, are subjected to mechanical stresses at their own weight, connection effects; the pipe elbow is a pipe connection. Regardless of the type of machinery, equipment and pipeline used, most of them are mainly used in oil transportation, gas transportation and bridge construction. Therefore, the effective boundary load analysis has attracted the attention of many researchers. In the study of Joong-Hyok et al (2), limit load solutions for pipe bends under combined bending and torsional moment are given. Studies by Marie et al. (3) analysed elastic stress solutions for 90° pipe bends under plane bending with a mean radius-to-thickness ratio of up to 50. Li et al. (4) investigated the load interaction behaviour of smooth pipe elbows with long straight pipes with defect by using a finite element method and then established the yield interaction behaviour when an elbow is subjected to a load combination in-plane bending, torsion and internal pressure. Karamanos et al. (5) analysed the nonlinear elastic–plastic response of 90 degree pipe bends under internal pressure under in-plane and out-of-plane bending. Cui et al. (6), investigated the influence of

torque and bending moment on the limiting internal pressure of bends with local wall thinning defects. Peng and Changyu (7) considered in their analysis the effect of local wall thinning (LWT) of the pipe subjected to different loads; pressure, bending moment and combined loads. They analysed the resistance of the pipe experimentally and numerically by the finite element method. The results showed that the influence of depth and circumferential length of LWT on the limit load is more evident compared to that of the axial length when an elbow is under pressure, bending moment or torque. Elbows are used in piping systems as they provide flexibility in response to thermal expansion and other loads that impose large displacements on the system.. As with most piping considerations, understanding the ideal uses of the elbow pipe in the application areas is essential for good design and for proper operation of the finished system. Therefore, there is a need to move towards new materials exhibiting high strength and thermal resistance when undergoing severe thermomechanical loads. To meet these requirements, the process of choosing and producing such materials must be improved. This is achieved by replacing existing conventional materials with such new generation materials. For this purpose, functional gradient materials are studied (8).

In recent years, functionally graded materials (FGMs) have attracted a lot of attention due to their many benefits. Functionally graded materials is an emerging field of research. FGMs with

brittle and ductile materials presented a rather important advantage in the application of the structures of high precision as well as those under mechanical loading. Therefore, current research is mainly centred on the discovery of the nature complex fracture mechanics due to the inhomogeneity of materials. From recently published work (9) a detailed analysis of functional gradient pipe bends under a bending moment was carried out using a finite element analysis of a numerical model. Dai et al. (10) presented the effect of the volumetric ratio of constituents and porosity on magnetoelastic stresses and perturbation of magnetic field vector and to design the optimum FGM cylindrical and spherical vessels. Yavar et al. (11) developed stress analysis of a functionally graded hyperplastic thick spherical shell subjected to internal and external pressures whose hyperplastic behaviour is modelled by using the modified neo-Hookean strain energy function with variable material parameters. Benslimane et al. (1) presented an analytical formulation to find displacements and stress components in thick-walled cylinder FGM subjected to internal and external pressures. Almasi et al. (12) developed an FGM cylindrical tube model for elastic limit domain assessment using an analytical solution. This tube undergoes internal pressure and temperature difference with superimposed heat generation. Nejad et al. (13) investigated the time-dependent thermoplastic creep response for isotropically rotating thick-walled cylindrical pressure vessels made of a functional gradient material (FGM), taking into account the creep behaviour of FGM pressure vessels. Using finite element analysis, damage problems of FGM structures have been widely studied in the literature. Lee and Toi (14) analysed the elastoplastic behaviour of FGMs subjected to thermal loading by using the finite element method using continuum damage mechanics (CDM). They used the Lemaitre damage model to analyse the damage behaviour of an FGM disk. They discussed the effect of FGM on thermal damage by some numerical examples for industrial materials. Thamburaj and Johnson (15) used a finite element model (LS-DYNA) to develop FGMs. The Johnson-Holmquist damage model (JH2 model) is used to predict and measure damage propagation in materials. Houari et al. (16) established a simple and efficient method using Matlab-UMM to model an FGM (Ti/TiB) according to several types of hardware designs and to compare the results to the classical ABAQUS method using UMAT (User Material). The meshing method (UMM) has been found efficient in the analysis of the elastic-plastic behaviour and damage of an FGM structure in the presence of a central circular notch. In another work, Houari et al. (17) authors analysed, by using the finite element method and the code of ABAQUS, the variation of the circular, radial and axial forces in a tubular structure in FGMs; it is assumed that that the used material is isotropic and heterogeneous, solicits only under the internal pressure. In our work, we proposed a multifunctional material graduated in 3D (which is new), that is to say the definition of the properties of the material by element molecular language, for the purpose of defining a resolution of a design produced by the Additive manufacturing method. To facilitate their use in various fields of specific application. Numerical studies on optimal vibration control of power law FGM (P-FGM) pipes subjected to a high-temperature environment are presented for different volume fraction indices of FGM.

2. MODEL GEOMETRIC

A bent pipe with an outside diameter of $D = 185.4$ mm is considered in this study, with the value of angle of curvature (devia-

tion) equal to 90. The thickness of the pipe is equal to 23.4 mm, corresponding to a diameter-to-thickness ratio (D/e) equal to 7.9. The radius-to-diameter ratio of the elbow (R/D) is equal to 1.34. The vertical system pipe of length $L = 727.5$ mm is embedded in a floor (Fig. 1). The pressure pipes are simulated, with an internal pressure equal to $P = 7$ MPa (70 bar), and the horizontal pipe part of length $l = 160$ mm was produced with a force of $F = 480$ N and a bending moment to $M_f = 200$ N. mm. The presence of a bend aims to concentrate the stresses and locate a plastification, which will act a source of initiation of damage.

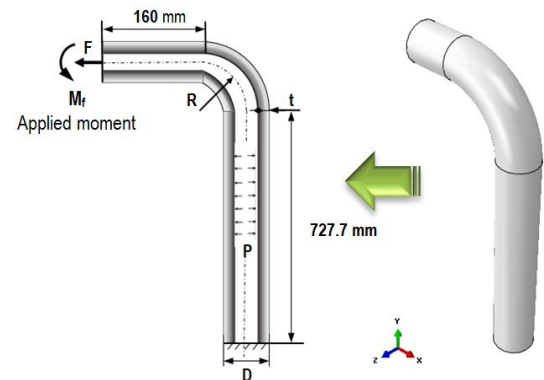


Fig. 1. Geometric model of a mass FGM cylinder

3. MATERIALS WITH PROPERTY GRADIENT (FGM Ti-TiB)

Metal/ceramic FGMs are becoming more and more important in modern technology; they are used to meet industrial requirements because they combine the properties of metals (ductility and high electrical and thermal conductivity) and the properties of ceramics (high hardness, resistance to corrosion and temperature). In addition, the presence of notches within the FGM constitutes not only a geometric discontinuity but also a source of crack initiation and stress concentration, which can damage the material with a property gradient with a brittle or ductile fracture. We used an FGM material (Ti titanium/TiB titanium monoborder). The FGM elbow pipe material is composed of two ductile/brittle materials (Ti/TiB); their material properties are defined in Table1.

Tab. 1. Material property [19]

Property	Metal Ti	Ceramic TiB
Young's modulus E	107,000 MPa	375,000 MPa
Poisson's ratio ν	0.34	0.14
Yield stress σ_Y	450 MPa	-
Ultimate tensile strength σ_{UTS}	552 MPa	1,400
Fracture energy G_{Ic}	24 KJ/m ²	0.11 KJ/m ²
Ratio of stress to strain transfer "q"	4,500 MPa	

4. ANALYTICAL FORMULATION

Most articles in the literature on FGMs use the simple mixing rule to obtain effective material properties. Regarding volume fraction distribution functions, the equivalent material properties of FGMs could be determined by various functions in power law FGM (P-FGM), sigmoid law FGM (S-FGM) or exponential law FGM (E-FGM) form. There are several types of homogenisation

methods. For example, the Voigt method, which is frequently applied in FGM analysis, estimates the material properties of FGMs, and the Mori–Tanaka model estimates the effective shear G and isostatic modulus of elasticity K of the FGM, Y. It should be noted that the effective material properties given by the Hashin–Shtrikman lower bound are equivalent to the Mori–Tanaka micro-mechanical model, and the upper bound can also be obtained by interchanging the matrix and including in the formulation of the Mori–Tanaka model [20]. Tamura et al.[21] proposed a simple model to describe the stress–strain curves of composite materials. The model has been used to predict elastic and plastic constitutive responses for a range of representative multiphase materials. TTO formulation reduces to Voigt’s estimate for $q_t = \pm\infty$ and the Reuss estimate for $q_t = 0$.

This part shows that the properties of FGM are continuously varied in their direction by row of finite elements according to the model used in this work – UMM, and this in accordance with the law of mixture. To determine the material properties of the elastic part of the FGMs, the Mori–Tanaka model was used to estimate the effective shear G and isostatic modulus of elasticity K of the FGM as follows:

$$K_{UMM}^k(r_i) = K_m + \frac{(K_c - K_m) \left(\frac{r_i - R_{in}}{R_{ex} - R_{in}}\right)^n}{1 + \left(1 - \left(\frac{r_i - R_{in}}{R_{ex} - R_{in}}\right)^n\right) \frac{3(K_c - K_m)}{3K_m + 4G_m}}$$

and

$$G_{UMM}^k(r_i) = G_m + \frac{(G_c - G_m) \left(\frac{r_i - R_{in}}{R_{ex} - R_{in}}\right)^n}{1 + \left(1 - \left(\frac{r_i - R_{in}}{R_{ex} - R_{in}}\right)^n\right) \frac{(G_c - G_m)}{G + f_1}} \quad (1)$$

$$f_1 = \frac{G_m(9K_m + 8G_m)}{6(K_m - 2G_m)} \quad (2)$$

Then, the effective value of Young’s modulus and Poisson’s ratio can be given as follows:

$$E_{UMM}^k(r_i) = \frac{9K_{UMM}^k(r_i)G_{UMM}^k(r_i)}{3K_{UMM}^k(r_i) + G_{UMM}^k(r_i)}$$

and

$$\nu_{UMM}^k(r_i) = \frac{3K_{UMM}^k(r_i) - 2G_{UMM}^k(r_i)}{2(3K_{UMM}^k(r_i) + G_{UMM}^k(r_i))} \quad (3)$$

where $E_{UMM}^k(r_i)$ is effective Young’s modulus of FGM of row k ; i is the surface number; the subscript k denotes the location of a row of graduated elements; the subscripts c and m represent the ceramic and metallic phases, respectively; R_{in} denotes the inner radius of the cylinder; R_{ex} is the outside radius of the cylinder; r_i is the coordinate of each surface along the radius; and n is the exponent of the non-negative volume fraction. On the other hand, the TTO model homogenisation formulations are used in the UMM method to determine the properties of the plastic part. The TTO model equations are as follows:

$$H_{UMM}^k(r_i) = \left[\left(H_m \frac{q+E_c}{q+H_m} - E_c \right) \left(\frac{r_i - R_{in}}{R_{ex} - R_{in}} \right)^n + E_c \right] / \left[\frac{q+E_c}{q+H_m} \cdot \left(\frac{r_i - R_{in}}{R_{ex} - R_{in}} \right)^n + \left(1 - \left(\frac{r_i - R_{in}}{R_{ex} - R_{in}} \right)^n \right) \right] \quad (4)$$

and

$$\sigma_{Y_0}^k(r_i) = \sigma_{Y_0m} \left[\frac{q+E_m}{q+E_c} \frac{E_c}{E_m} \cdot \left(1 - \left(\frac{r_i - R_{in}}{R_{ex} - R_{in}} \right)^n \right) + \left(\frac{r_i - R_{in}}{R_{ex} - R_{in}} \right)^n \right] \quad (5)$$

We propose

$$r_i = \Delta r_k (i - 1) + R_{in}$$

where $\sigma_{Y_0}^k(r_i)$ is the row FGM yield strength and $k \sigma_{Y_0m}$ is the yield strength of the metal and H_m tangent modulus of the metal.

The proposed criterion to predict FGM damage in our case of combined internal pressure and bending moment (Fig. 2). They rest on one or the other of the conditions of maximum deformation for initialisation of damage. The approach to predict the maximum deformation of FGM $\epsilon_{UTS}(r)$ is shown in the following equation:

$$\epsilon_{UTS}(r_i) = \epsilon_{UTSm} \cdot \left[\frac{q+H_m}{q+E_c} \cdot (1 - V_m) + V_m \right] \quad (6)$$

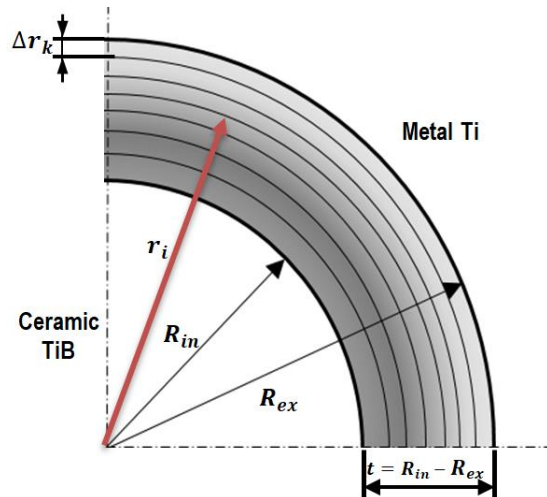


Fig. 2. Illustration of layers in an FGM (TiB/Ti) pipe

The MAXPS criterion as shown in the following equation:

$$w = \frac{\epsilon_{eq}}{\text{Avg} \sum \epsilon_{UTS}^k(r_i)} = 1 \quad (7)$$

where ϵ_{UTSm} denotes the maximum deformation of metal, H_m is the tangent modulus of metal, $\Delta \epsilon^-$ is the accumulated increment of the equivalent plastic strain of the FGM during an integration step, $\bar{\epsilon}_f^{pl}$ is the equivalent strain of the FGM at failure and w is the damage parameter for failure initiation when it is equal to 1. The evolutions of the damage are defined by the energy condition to create new free surfaces (Eq. 2). The choice of the energy approach is often governed by the size of the finite elements.

$$G_f^k(r_i) = \int_{\bar{\epsilon}_f^{pl}}^{\bar{\epsilon}_f^{pl}} L \sigma_{Y_0}^k(r_i) d\bar{\epsilon}^{pl} \quad (8)$$

Thus, following the initiation of the damage, the variable of damage increases according to the following equation:

$$D = \frac{L d\bar{\epsilon}^{pl}}{\bar{u}_f^{pl}} \quad (9)$$

where \bar{u}_f^{pl} is the equivalent plastic displacement at failure of the FGM, which is calculated as in the following equation:

$$\bar{u}_f^{pl} = \frac{2 \cdot \text{Avg} \sum G_f^k(r_i)}{\text{Avg} \sum \sigma_{Y_0}^k(r_i)} \quad (10)$$

where $\sigma_{Y_0}^k(r_i)$ is the elastic limit of the FGM, $G_f^k(r_i)$ is the fracture energy of the FGM and L is the characteristic of the finite element.

5. FORMULATION OF FINITE ELEMENTS

The main feature of FGM is that it gradually changes inside the structure. This distribution of materials makes it possible to modify the properties inside the structure. Gradients of properties can thus be achieved at the mechanical, physical, chemical levels, etc. The main goal of the mechanics of materials is to predict the behaviour of materials. This requires estimating the effective mechanical properties of the two-phase composition, which is commonly referred to as homogenisation. Therefore, the analysis of FGM components involves two important aspects: the definition of the volume fraction at each point of the component and the evaluation of the effective composite properties at each point from the properties and volume fractions of each phase. In the numerical simulation, there are various possibilities of modelling the bent pipe in the ABAQUS/standard calculation code. In most studies in the literature, the pipe bend was also performed as part of the explicit calculation [5,7]. This method works, but it is relatively expensive. A much more efficient approach, which is simple in ABAQUS/standard and has been applied in this study, is the implicit–explicit coupling. The internal pressure is taken into account in a calculation step with ABAQUS/implicit, which takes only a few minutes, and then the model and the stress state are transferred to a calculation with ABAQUS/explicit for the bending moment.

We used a homogenization model (TTO) in the form of a

$$[C_{UMM}^k] = \begin{bmatrix} \lambda(r) + 2G(r) & \lambda(r) & \lambda(r) & 0 & 0 & 0 \\ \lambda(r) & \lambda(r) + 2G(r) & \lambda(r) & 0 & 0 & 0 \\ \lambda(r) & \lambda(r) & \lambda(r) + 2G(r) & 0 & 0 & 0 \\ 0 & 0 & 0 & G(r) & 0 & 0 \\ 0 & 0 & 0 & 0 & G(r) & 0 \\ 0 & 0 & 0 & 0 & 0 & G(r) \end{bmatrix} \quad (12)$$

For the UMM method, the MATLAB program was used to determine all the values of the mechanical properties of FGM for each row of finite elements according to its location and its gradation in the structure according to the TTO model. The purpose of this technique is to introduce the values of the mechanical properties of FGM directly into the ABAQUS computer code.

The UMM technique allows determining finite element stiffness equations by principle of virtual work, and the stresses for each row of finite elements can be given in the following form:

$$\sigma_{UMM}^k = [C_{UMM}^k][B]\{u_n\} \quad (13)$$

where σ_{UMM}^k is the constraint of each range, C_{UMM}^k is the elasticity matrix of each range k and u_n is the classic displacement field. For this purpose, Hooke's law is used to determine the stresses at the macroscopic levels:

$$\sigma_{UMM} = Avg \sum \{\sigma_{UMM}^k\} = Avg \sum [C_{UMM}^k] [B]\{u_n\} \quad (14)$$

$$F_{UMM}^{FGM} = \int_V [B]\{\sigma_{UMM}\}dV \quad (15)$$

The technique of XFEM, which exists in the code ABAQUS, is compatible with the finite elements of the technique of mesh UMM in the structures out of materials with functionally graded (FGM). At the same time, the use of the method of XFEM to face a numerical difficulty that of the phenomenon of volumetric closure due to the incompressibility in plasticity.

$$u^h(x) = \sum_{i \in N} N_i(x)u_i + \sum_{i \in N_d} N_i(x)H(x)a_i + \sum_{i \in N_p} N_i(x) \left(\sum_{j=1}^4 F_j(x)b_i^j \right) \quad (16)$$

power law. The effective material properties of the FGM bent pipe are obtained for each volume fraction and have been determined by the Abaqus computer code using the UMM mesh method based on the size of the finite elements.. It should also be noted that the choice of elements for the discretisation of the structure is essential for the study of the damage of structure FGM.

The UMM technique is conditioned by the type of 3D solid finite element and the size of the finite elements in the direction of gradation. The structure is modelled by solid elements with eight nodes (C3D8R). So, all the FGM (ceramic/metal) models are analysed with the same type of the solid element C3D8R and with the same number of 100,000; the details are presented in Fig. 3. The UMM technique was used to determine the mechanical properties of FGM in element code finite ABAQUS, and the formulation of the approach is as follows:

$$P_{UMM}^k = \sum_{j=1}^m \sum_{i=1}^8 P_i^j N_i \quad (11)$$

where (i) represents number of nodes per element $i = 1,8$ and P_{UMM}^k is the property of FGM of the row or « m » expresses the number of identical elements in each row (Fig. 2).

Afterwards, the formula of the UMM method can determine the two lame coefficients $\lambda(r)$ and $G(r)$, which are expressed as a function of Young's modulus of composite $E(x)$ and Poisson's ratio $\nu(r)$; then the relation of tensions and stresses are deduced from the constitutive law using the 3D elasticity matrix from these equations:

where u_i is the classic displacement field at the node i , $N_i(x)$ is shape function, a and b are the corresponding degrees of freedom, $H(x)$ is the heaviside type enrichment function and $F_i(x)$ is the enrichment function. The final equation is as follows:

$$\sigma_{UMM} = Avg \sum \{\sigma_{UMM}^k\} = Avg \sum [C_{UMM}^k] [B]\{u^h\} \quad (17)$$

6. RESULTS AND ANALYSES

6.1. Mesh sensitivity

This part aims to validate the numerical model chosen for the analysis by highlighting the effect of the density of mesh elements on the convergence of the results. Indeed the density of mesh must be appropriate to have good results compared to the practice or compared to the stability of the results. The choice of solid finite element type C3D8R in our study aims to create a row of the same type of element. Consequently, the UMM/USDFLD method consists in integrating the distribution of the mechanical properties of the different constituents of the FGM-type ceramic/metal by row of finite elements in all directions of the structure in 3D with a type of hexahedral element C3D8 (see Fig. 3.). Our choice was the type of hexahedral element C3D8R, which is widely used in the mesh of structures; however, the number of type of mesh elements has been varied (see Fig. 4.). We also used all the densities of mesh to determine their effects on the stability of the results

by the curves of traction in the form force*–displacement. From the determined tensile curves, it was possible to demonstrate the effect of the mesh density in relation to the ultimate tensile force in the pipe elbow oriented at 90°.

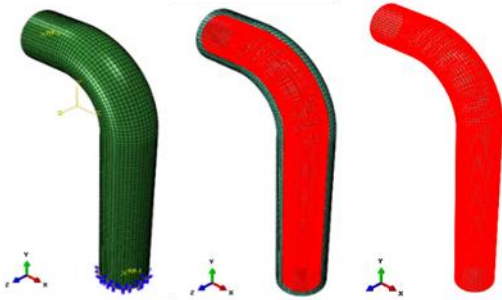


Fig. 3. Description of the mesh according to the material property variation of the FGM (TiB/Ti) per row

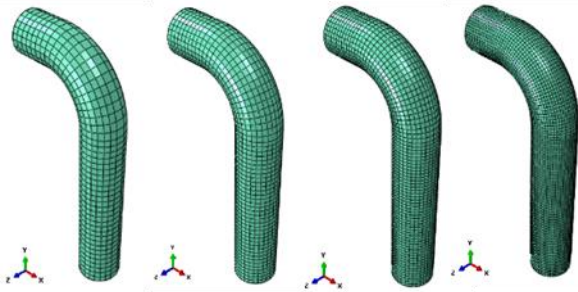


Fig. 4. Presentation of the mesh density in the 90° pipe bend: (a) 13,000 FE, (b) 22,500 FE, (c) 45,000 FE, (d) 100,000 FE

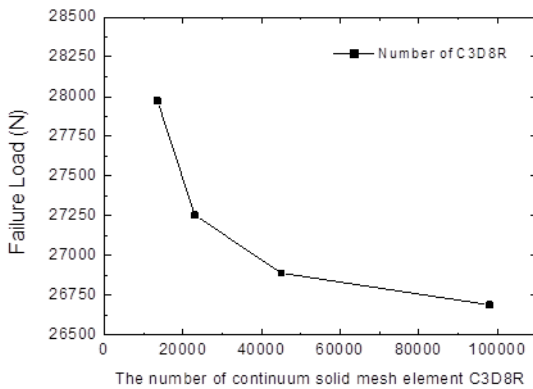


Fig. 5. Effect of the mesh element density on the response in the force–displacement tensile curve with respect to the pipe bend oriented at 90° under in-plane bending in metal Ti

Fig. 5 represents the tensile force–displacement curve of the 90° Ti metal pipe bend as a function of the different number of mesh elements. It can be noticed that compared to the elastic part, the density of elements does not have an influence on the variation of the curve force–displacement. On the other hand, the density of elements of mesh has an influence on the plastic part, or there can be a slight variation in the force according to the number of elements chosen for the mesh of the structure. From the tensile curves shown in Fig. 5, it was possible to represent the variation of the ultimate tensile force in the metal 90° pipe bend under in-plane bending as a function of mesh element density

(Fig. 6). The resistance of the bend on the metal part which has a plastic part clearly depends on the density of the mesh elements. It is preferable to have a structure discretised in a maximum number of elements (refined structure). The maximum value of the force determined numerically presents a value close to that found experimentally for the metal Ti (see Tab. 1 [19]).

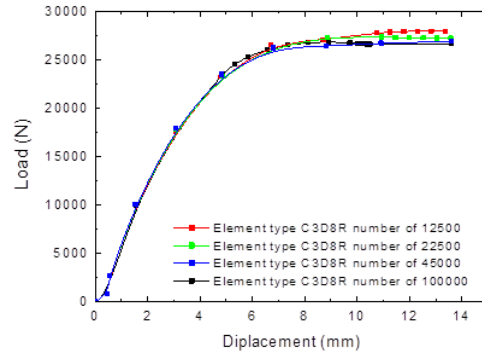


Fig. 6. Variation of maximum tensile strength of 90° pipe bend under in-plane bending in metal Ti as a function of mesh density

Another important parameter that was the subject of our sensitivity analysis is the number of surfaces introduced into the structure and the number of points of Gauss between these surfaces with the UMM technique. Our analysis of the effect of the density of mesh elements has no influence on the geometric approach to gradation but essentially on the behaviour to damage such as crack initiation and propagation. Element C3D8R has to demonstrate its performances in the comparison of the results with the experimental results; in the same way, this type of element is appropriate with the criterion of the evolution of damage and is known by these advantages with the use of XFEM [18].

6.2. The effect of gradation exponent on structural strength in FGM

In Fig. 7, we can notice if the structure is in rotation with respect to the axis xx , and that if $n = 0.5$, the pipe is rich in metal. The overall elongation of the bent pipe presents more plasticity with a maximum elongation. If the volume fraction exponent increases, the bent pipe becomes ceramic-rich and thus more strength and less ductility. An increase in the gradation exponent leads to an increase in the maximum force value of almost 4,500 N, which is beneficial for the structure.

If there is a rotation around the YY axis, the same phenomenon is observed, except that the value of the maximum force decreases considerably for an exponent of gradation equal to 2, where the structure is rich in ceramics. At this rotation, the structure has good resistance in terms of force and displacement for a balanced gradation coefficient equal to 1 and hence a linear distribution. If the elbow structure is rich in metal, the strength of the structure will be low.

If the structure is imposed on a rotation along the YY axis, the resistance of the elbow will be low and clearly lower than that when the rotation is imposed along the XX axis (Fig. 7). The effect of the gradation coefficient is important for the strength of the structure; if this coefficient has a low value (structure rich in metal), the structure has a very low resistance. However, if the structure is rich in ceramics, ie the gradation coefficient is high, it has good resistance but with low displacement.

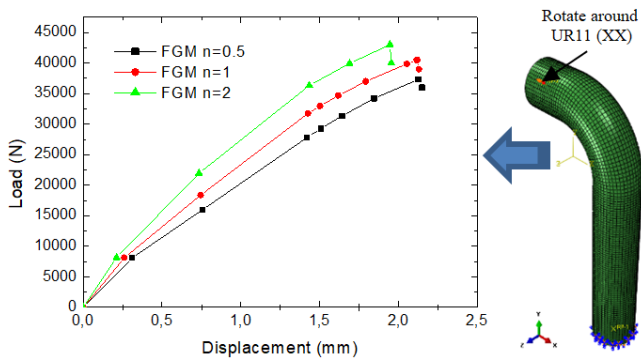


Fig. 7. Force–displacement of the pipe bent at 90 in FGM (TiB/Ti) with different exponents $n = 0.5, 1$ and 2 , ratio condition ($D/t = 7.9$) and rotate around UR11 (XX)

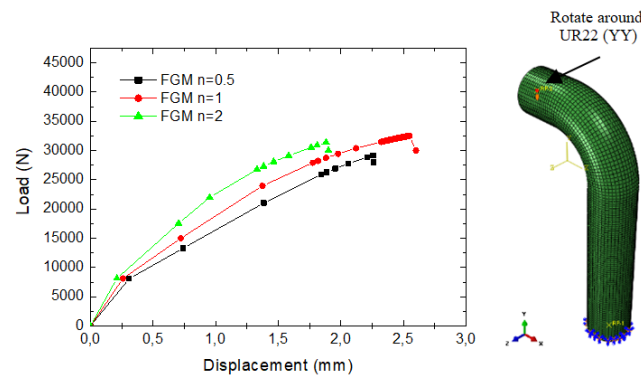


Fig. 8. Force–displacement of the pipe bent at 90 in FGM (TiB/Ti) with different exponents $n = 0.5, 1$ and 2 , ratio condition ($D/t = 7.9$) and rotate around UR22 (YY)

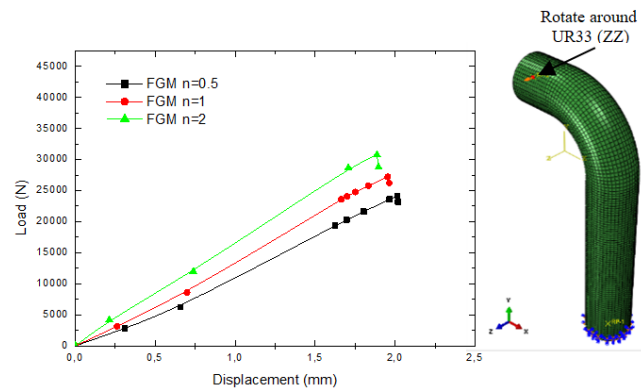


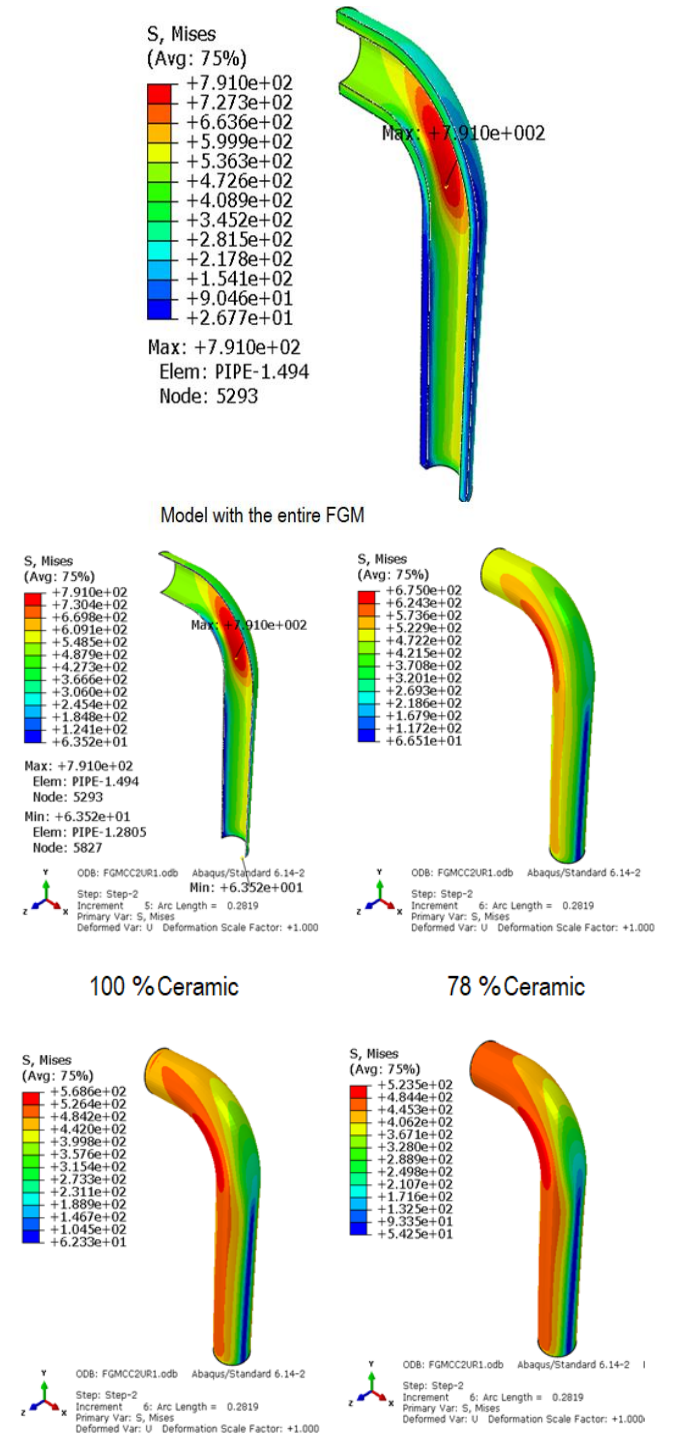
Fig. 9. Force–displacement of the pipe bent at 90 in FGM (TiB/Ti) with different exponents $n = 0.5, 1$ and 2 , ratio condition ($D/t = 7.9$) and rotate around UR33 (ZZ)

If one imposes a bending according to the axis ZZ, the structure presents one more weak resistance than when at the two other axes (Figs. 7 and 8). Similarly in Fig. 9, the effect of the gradation coefficient is importance for the resistance of the structure. The structure presents damage if a bending moment is imposed with respect to this direction.

6.3. Maximum stress analysis of bent pipe case $n = 2$ and moment around the axis (XX)

The analysis of the maximum stress level in the bent structure shows heterogeneity in the stress distribution at each layer of the

structure (Fig. 10). At the level of the internal radius where the ceramic-rich structure, it is clearly noticed that the maximum stress is at the level of the elbow on a very wide zone where the radius is minimal. Therefore, going outward from the bend, a significant concentration of stresses due to the simultaneous application of pressure and bending. Each layer of the FGM pipe has a different distribution depending on the % of each material. maximum stress is in the ceramic-rich part 791 MPa.. Towards the metal-rich part, there is more stress concentration zone but with lower stress values. For this load case, the stress in the metal part almost reaches the zone elastoplastic onset point of 454.2 MPa.



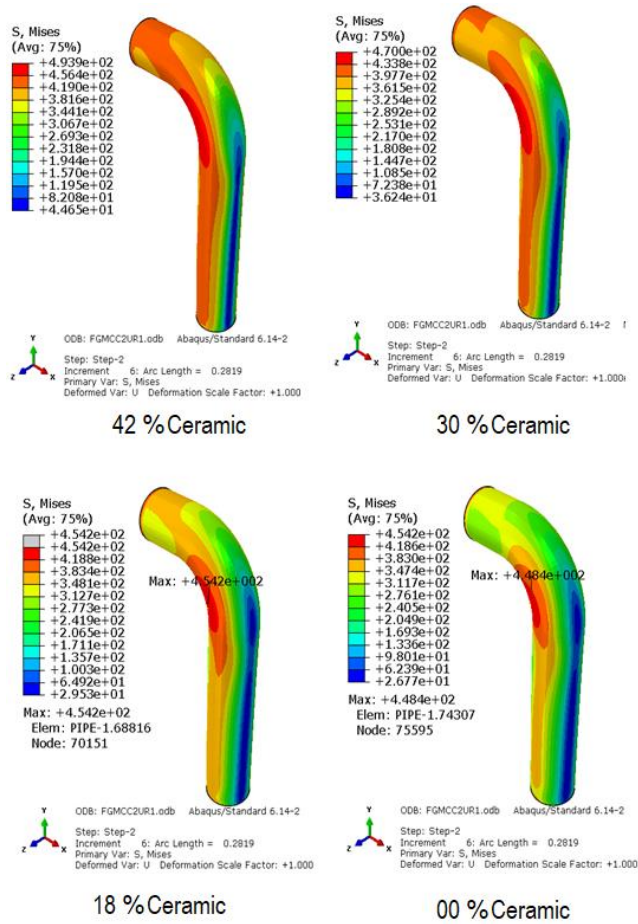


Fig. 10. Maximum stress analysis of bent pipe case exponent $n = 2$ and moment around axis UR11 (XX)

6.4. Crack initiation case $n = 2$ (rich ceramic) and moment around the axis (XX)

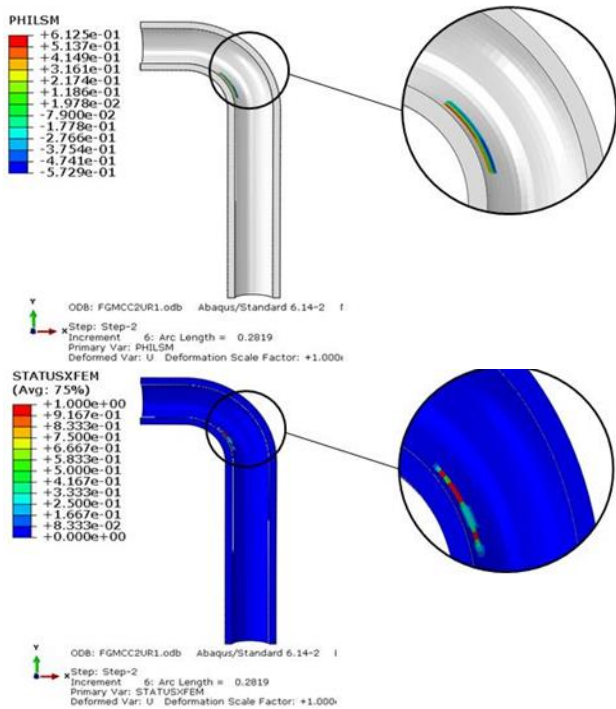


Fig. 11. Initiation of the crack case exponent $n = 2$ (rich ceramic) and moment around the axis UR11 (XX)

Fig 11 shows the path of the crack. We notice at this part a force zone of stress concentration causing the initiation of the crack. For this value of gradation coefficient with a moment around the (XX) axis, it is better to optimise the distribution of the two materials according to a new design.

6.5. Deformation of the structure with the case $n = 2$ (rich ceramic inside elbow) and moment around the axis (XX)

Fig. 12 shows the distorted circular shapes for elbows ($D/t = 7.9$ and $R/D = 1.34$) under in-plane bending around the XX axis of closing and opening.

It is clearly noted that for this rotation along the xx axis, the structure presents more deformation on the upper part of the elbow at the level of the metal face and slight concentration of stress at the level of the ceramic face, while the rest of the structure has good resistance.

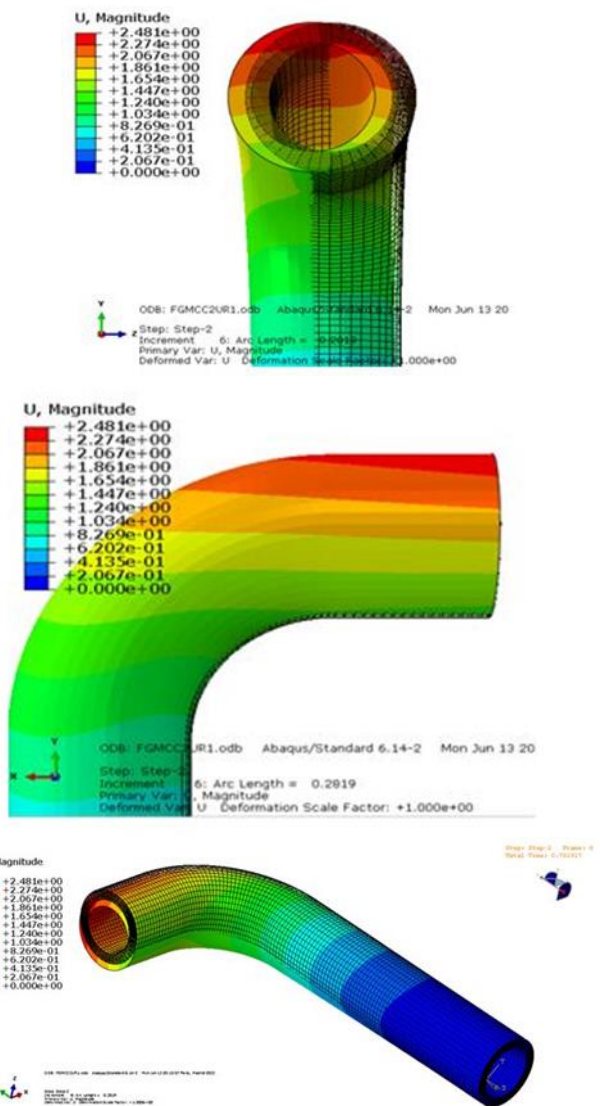


Fig. 12. Distorted circular shapes for elbows ($D/t = 7.9$ and $R/D = 1.34$) under in-plane bending around the XX axis of closing and opening

6.6. Moment effect around the axes

The determination of the variation of the bending moment as a function of the angle of rotation of the structure is essential to have an idea of the resistance of the elbow.

It is clearly noticed from Fig. 13 that regardless of the direction of rotation of the structure (according to XX or YY or ZZ) the value of the bending moment varies practically in the same way with the angle of rotation.

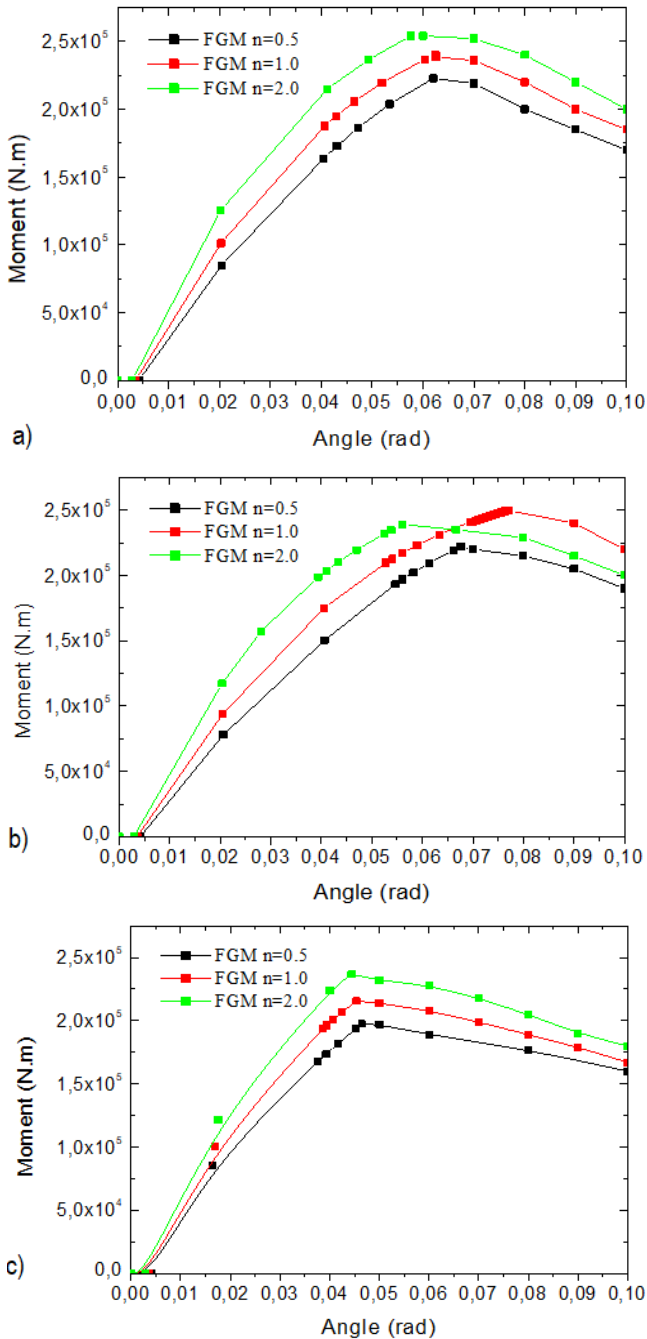


Fig. 13. Moment–rotation diagram of elbows under bending in the presence of external pressure, effect around the axes: (a) FGM-UR11, (b) FGM-UR22, (c) FGM-UR33

For the rotation along XX (Fig. 13a), the maximum value of the moment is reached for a rotation angle value equal to 0.06 rad and for the case where the structure is rich in ceramics. On the

other hand, if the rotation takes place along the YY axis (Fig. 13b), the maximum value of the moment is reached for an angle equal to 0.075 for the case where the gradation coefficient is equal to 1. Consequently, for the case where the rotation is the ZZ axis (Fig. 13c), the maximum value of the moment is reached quickly for an angle equal to 0.045 and for the case where the structure is rich in ceramics. If the structure is rich in metal, the value of the bending moment is low, and this applies for all cases of rotation along different axes.

7. CONCLUSION


Once a crack is initiated, the structure becomes weak in terms of strength, giving rise to a significant deformation of the structure at the most stressed area (i.e. elbow). The spatial and progressive variations of the properties of FGM make it possible to propose gradation concepts for innovative structures that can be exploited in many fields of application. The UMM technique gives us the advantage of varying more than two materials in the FGM. The present work has demonstrated the effectiveness of the numerical results with the proposed UMM technique with respect to the damage of a bent FGM pipe structure.


- The optimisation of the gradation coefficient provides better resistance to the structure.
- According to the direction of bending (rotation of the structure), the exponent of gradation presents an important factor in the structure in terms of force displacement.
- According to the rotation XX, for a gradation coefficient $n = 2$, the structure presents a better resistance. On the other hand, if the stress is along the YY axis, the gradation coefficient $n = 1$ presents a better resistance of the structure in terms of force and elongation.


REFERENCES

1. Benslimane A, Bouzidi S, Methia M. Displacements and stresses in pressurized thick-walled FGM cylinders: Exact and numerical solutions. *Int. J. Press. Vessel.* 2018 December; 168: 219-224. <https://doi.org/10.1016/j.ijpvp.2018.10.019>.
2. An J, Hong P, Kim J, Budden J. Elastic stresses for 90° elbows under in-plane bending. *Int. J. Mech.* 2011;53(9): 762-776. <https://doi.org/10.1016/j.ijmecsci.2011.06.008>.
3. Marie S, Chapuliot S, Kayser Y, Lacire MH, Drubay B:BB, Triay M. French RSE-M and RCC-MR code appendices for flaw analysis: Presentation of the fracture parameters calculation—Part I: General overview. *Int. J. Press. Vessel.* 2007 October–November; 84(10–11): 590-600. <https://doi.org/10.1016/j.ijpvp.2007.09.001>.
4. Li Y, Gao B, Liu S, Ding J. Finite Element Analysis of the Limit Load of Straight Pipes with Local Wall-Thinning Defects under Complex Loads. *Appl. Sci.* 2022 Novembre; 12(10): 4850; <https://doi.org/10.3390/app12104850>.
5. Karamanos SA, Tsouvalas D, Gresnigt AM. Ultimate Bending Capacity and Buckling of Pressurized 90 deg Steel Elbows. *J. Press. Vessel Technol.* 2006; 128: 128–356..
6. Bao S, Liu Y, Mao J, Ge R, Li X. Numerical and experimental investigation on limit load of elbow with local thinning area. *International Journal of Pressure Vessels and Piping.* 2019 May; 172: 414-422. [doi:10.1016/j.ijpvp.2019.04.014](https://doi.org/10.1016/j.ijpvp.2019.04.014).

7. Peng C, Changyu Z. Limit Load Analysis of Elbow with Local Wall Thinning under Combined Loads. *Applied Mechanics and Materials*. 2015 April ; 750: 198-205.
<https://doi.org/10.4028/www.scientific.net/AMM.750.198>.
8. Ansari S, Rahimi G, Citarella R, Shahbazi K, Sepe R, Esposito.. Analytical solutions for yield onset achievement in FGM thick walled cylindrical tubes undergoing thermomechanical loads. *Composites Part B: Engineering*. 2017 May; 116: 211-223.
<https://doi.org/10.1016/j.compositesb.2017.02.023>.
9. Lee KH, Oh CS, Kim YJ, Yoon KB. Quantification of the yield strength-to-elastic modulus ratio effect on TES plastic loads from finite element limit analyses of elbows. *Engineering Fracture Mechanics*. 2009 May ; 76 (7): 856-875.
10. Dai HL, Fu YM, Dong Z. Exact solutions for functionally graded pressure vessels in a uniform magnetic field. *International Journal of Solids and Structures*. 2006 September; 43(18–19): 5570-5580.
<https://doi.org/10.1016/j.ijsolstr.2005>.
11. Yavar A, Gholamhosein R.. Stress analysis of thick pressure vessel composed of functionally graded incompressible hyperelastic materials. *International Journal of Mechanical Sciences*. 2015 decembre ; 104 : 1-7. <https://doi.org/10.1016/j.ijmecs>.
12. Almasi A, Baghani M, Moallemi A. Thermomechanical analysis of hyperelastic thick-walled cylindrical pressure vessels, analytical solutions and FEM. *International Journal of Mechanical Sciences*. 2017 September ; 130: 426-436.<https://doi.org/10>.
13. Nejad Z, Kashkoli D. Time-dependent thermo-creep analysis of rotating FGM thick-walled cylindrical pressure vessels under heat flux. *International Journal of Engineering Science*. 2014 September ; Volume 82: 222-237.<https://doi.org/10.1016/j.ijengs>.
14. Lee M, Toi Y. Elasto-plastic damage analysis of functionally graded material disks subjected to thermal shock and thermal cycle. *Nippon Kikai Gakkai Ronbunshu, A Hen*. 2001 ; 67(655): 503-510.
15. Thamburaj P, Johnson W. Propagation of Damage in Functionally Graded Materials under Impact Loads. In 47th AIAA/ASME/ASCE/AHS/ASC Structures, Structural Dynamics, and Materials Conference 14th AIAA/ASME/AHS Adaptive Structures Conference 7th. 2012 Jun ;; <https://doi.org/10.2514/6.2006-2012>.
16. Houari A, Mokhtari M, Bouchikhi A, Polat A, Madani K. Using finite element analysis to predict the damage in FGM-3D notched plate under tensile load; Different geometric concept. *Engineering Structures*. 2021 15 June; 237: 112-160.
<https://doi.org/10.1016/j.engstruct.2021.112160>.
17. Houari A, Mokhtari M, Bouchikhi A, Polat A, Madani K. Numerical analysis of the elastic-plastic behavior of a tubular structure in FGM under pressure and defect presence. *Frattura ed Integrità Strutturale*. 2022; 16(59): 212–231. doi: 10.3221/IGF-ESIS.59.1.
18. Jin Z, Paulino G, Dodds R. Cohesive fracture modeling of elastic–plastic crack growth in functionally graded materials. *Engineering Fracture Mechanics*. 2003 September; 70(14): 1885-1912.
[https://doi.org/10.1016/S0013-7944\(03\)00130](https://doi.org/10.1016/S0013-7944(03)00130).
19. Mori T, Tanaka K. Average stress in matrix and average elastic energy of materials with misfitting inclusions. *Acta Metallurgica*. 1973 May ; 21(5): 571-574.[https://doi.org/10.1016/0001-6160\(73\)90064-3](https://doi.org/10.1016/0001-6160(73)90064-3).
20. Tamura Y, Tomota H, Ozawa.. Strength and Ductility of Iron-Nickel-Carbon Alloys Composed of Austenite and Martensite with Various Strength. *Proceedings of the 3rd International Conference on Strength of Metals and Alloys*, Cambridge. 1973 August ; 611.

 Amin Houari:  <https://orcid.org/0009-0004-2617-2182>

 Kouider Madani:  <https://orcid.org/0000-0003-3277-1187>

 Salah Amroune:  <https://orcid.org/0000-0002-9565-1935>

 Leila. Zouanbi:  <https://orcid.org/0000-0002-1732-5237>

 Mohamed Elajrami:  <https://orcid.org/0000-0003-0928-6124>


This work is licensed under the Creative Commons BY-NC-ND 4.0 license.